Numerical Analysis and Predictive Modeling Using Artificial Intelligence of the Relaxation Zone Around Hangingwall of Sublevel Open Stopes in Underground Mines

Amine Soufi*, Youssef Zerradi, Mohammed Souissi, Latifa Ouadif, and Anas Bahi

Mohammed V University in Rabat, Morocoo

Article Info	Abstract
	The aim of this study is to thoroughly analyze the relaxation zone developing around sublevel stopes in underground mines and identify the main parameters controlling its extent. A numerical approach based on the finite element method, combined with the Hoek-Brown failure criterion, was implemented to simulate various geometric configurations, geological conditions, and in-situ stress states. A total of 425 simulations were carried out by varying depth, horizontal-to-vertical stress ratio (k), rock mass quality (RMR), foliation orientation and spacing, as well as the height, width, and inclination of the sublevels. The results enabled the development of robust predictive models using regression analysis techniques and artificial neural networks (ANNs) to estimate the extent of the relaxation zone as a function of the different input parameters. It was demonstrated that depth and the k ratio significantly influence the extent of the relaxation zone. Additionally, a decrease in rock mass quality leads to a substantial increase in this zone. Structural characteristics, such as foliation orientation and spacing, also play a decisive role. Finally, the geometric parameters of the excavations, notably the height, width, and inclination of the sublevels, directly impact stress redistribution and the extent of the relaxation zone. The overall ANN model, taking into account all these key parameters, exhibited high accuracy with a correlation coefficient of 0.97. These predictive models offer valuable tools for optimizing the design of underground mining operations, improving operational safety, and increasing productivity.

1. Introduction

The underground mining of vein deposits poses considerable challenges in terms of hanging wall stability. Among the various techniques used, the sublevel stopping mining method occupies a prominent place, particularly for the extraction of sub-vertical deposits. However, this method is often confronted with recurrent hanging wall instability issues at the roof level (hanging wall), leading to major risks for worker safety and substantial productivity losses. These instabilities mainly result from the complex stress redistribution around underground empty chambers, itself influenced by numerous geological, geomechanical, and operational factors [1].

The quality of the rock mass, generally evaluated using empirical classifications such as the Rock Mass Rating (RMR), is another determining factor. A low-quality rock mass, exhibiting numerous discontinuities and low compressive strength, will tend to develop a more significant relaxation zone around excavations due to its greater deformability and lower capacity to redistribute stresses [2]. The structural characteristics of the rock mass, such as the orientation, spacing, and persistence of discontinuities (bedding, foliation, fractures), can also significantly influence hanging wall stability and the extent of the relaxation zone. Unfavorably oriented discontinuities relative to the hanging

✉ *Corresponding author: amine.soufi@outlook.com (A. Soufi).*

walls of sublevels stope can act as preferential sliding surfaces, thus promoting instabilities [3].

This study aims to analyze the relaxation zone around the hanging wall of sublevel open stopes in underground mines and develop predictive models using numerical methods and artificial intelligence techniques. Several works from the given articles are relevant to this study. These studies employ analytical methods, finite element methods (FEM), and numerical techniques such as multilayer perceptron (MLP) to analyze the contact lengths, contact pressures, and contact areas. Although the problem domains are different, the use of numerical methods and their validation with analytical solutions or FEM [1, 2, 9].

Other works investigate contact problems or surface interactions but focus on different materials or applications. While the problem domains differ, these articles demonstrate the application of numerical methods and ANNs in solving various engineering problems [3, 5, 8].

Some studies focus on the vibration and buckling analysis of functionally graded (FG) beams or porous beams using analytical, FEM, and ANN methods; these studies showcase the use of numerical methods and ANNs in analyzing the behavior of materials or structures under various conditions, which is relevant to the analysis of the relaxation zone in underground mines [4, 6].

Another work investigates the impact of material and flow properties on fluid-structure interaction in cage systems using FEM and computational fluid dynamics (CFD) methods. While the problem domain is different, this article demonstrates the use of numerical methods in analyzing complex structural behavior under various loading conditions, which is relevant to the analysis of stress redistribution and the relaxation zone in underground mines [7].

One study presents a mixed finite element model for the analysis of shallow footings rested on tensionless foundations, considering the out-of-plane components of the stress tensor. Although the problem domain is different, this article highlights the importance of considering appropriate stress components and modeling techniques in structural analysis, which is relevant to the analysis of the relaxation zone in underground mines [11].

Several studies have highlighted the importance of investigating the mechanical behavior of rock masses and the factors influencing their deformation and failure mechanisms. Numerically simulating the tensile behavior of transversely isotropic rocks using the discrete element method, considering the effect of anisotropy and loading rates, provides insights into the behavior of such materials [12]. Investigating the shear properties of open non-persistent latitudinal discontinuities, focusing on the influence of rock bridge area and number on shear strength, enhances the understanding of the role of structural discontinuities in rock masses [13]. Examining the failure mechanism of rock pillars containing edge notches through experimental tests and numerical simulations demonstrates the impact of notch angles on fracture patterns and failure mechanisms, highlighting the importance of considering structural discontinuities in rock masses [14].

Presenting experimental and numerical approaches to determine the fracture toughness and fracture energy of materials like oil well cement sheath using testing methods such as the hollow center cracked disc (HCCD) test and the cracked straight through Brazilian disc (CSTBD) test showcases the influence of notch length on fracture behavior and the applicability of different testing methods [15]. Describing the preparation of heterogeneous rock-like samples containing non-persistent notches emphasizes the importance of sample preparation techniques for laboratory investigations of rock mechanics [16]. Experimentally investigating the deformation behavior of circular underground openings in hard soil using a 3D physical model provides insights into the behavior of underground excavations and the effects of tunnel drilling, support systems, and surface loading on strata deformation and subsidence [17].

While previous studies have investigated individual factors or employed analytical or empirical approaches, this research utilizes a rigorous numerical approach based on the finite element method, combined with the Hoek-Brown failure criterion, to simulate various geometric configurations, geological conditions, and in-situ stress states. By systematically varying parameters such as depth, horizontal-to-vertical stress ratio, rock mass quality, foliation orientation and spacing, as well as the height, width, and inclination of the sublevels, the study aims to provide a complete evaluation of the relaxation zone and identify the predominant parameters controlling its extent. The development of robust predictive models using regression analysis techniques and artificial neural networks (ANNs) distinguishes this work, offering valuable tools for optimizing the design of underground mining operations, improving operational safety, and increasing productivity.

2. Methodology
2.1. Mining Method

The mining methods used at the Hammam mine in Morocco include sublevel stopping and overhand cut-and-fill mining. The stope is oriented in the East-West direction with a dip of 75°, 3.5 to 7 m wide, and 60 m long along the strike. Parallel blast hole rings were fired in a 3 m extracting height along a horizontal layer with multiple ring sequences. The stope was filled after every layer of mining, a typical mining arrangement. Hanging wall falls occurred in a variety of circumstances, which interrupted normal operations.

The most prevalent geometric configuration of sublevel open stopes at the mine site is depicted in Figure 1. However, several vein-type mineralized structures exist within the El Hammame mine, Morocco. To comprehensively address all possible scenarios and determine the relaxation zone extent for these structures across varying rock mass qualities, we conducted a parametric study considering all potential geometries for these sublevel stopes and estimating the relaxation arc along the Hanging wall. This approach ensures a thorough evaluation, encompassing the diverse array of geological conditions and excavation geometries encountered throughout the mine's operations. By systematically analyzing the influence of each parameter, our research aims to develop robust predictive models capable of accurately quantifying the relaxation zone magnitude, thereby optimizing stope design and enhancing excavation stability in this challenging underground mining environment. The rock mass characteristics and discontinuity patterns in the El Hammam district are as follows:

Ductile Deformations:

- The region shows schistosity (flat-lying planar fabrics) resulting from the Hercynian orogeny, especially the post-Visean phases.

- The rock formations are affected by significant NE-SW trending folding related to NW-SE compression, forming anticlines and synclines.

- The schistosity generally trends E-W to NE-SW with steep dips (45-80°) towards NW or N, suggesting the main Hercynian deformation direction was NW-SE.

Brittle Deformations:

- The district is highly fractured, with fracture directions varying from NE-SW to E-W.

- Three main fracture families are identified:

- NE-SW faults (hosting the mined fluorite veins), which are most important and correspond to the El Hammam/Filon3 fault zone, affecting most formations.

- E-W faults, often associated with tourmaline structures containing tin mineralization.

- N-S faults with sinistral displacements.

The mineralized fluorite veins are emplaced along the NE-SW fracture system, forming a major N45° shear corridor.

Structural Analysis:

- The fluorite veins delineate a mega-shear corridor trending N45°.

- The fluorite structures correspond to pull-apart lenses related to dextral transtensional movement along the major N45° faults, with normal faults and NW-plunging (30°NW) slickenlines.

The rock mass characteristics, including schistosity and folding from the Hercynian orogeny, as well as the brittle deformations with a major NE-SW shear corridor, play a key role in controlling the discontinuity patterns and fluorite mineralization in the district.
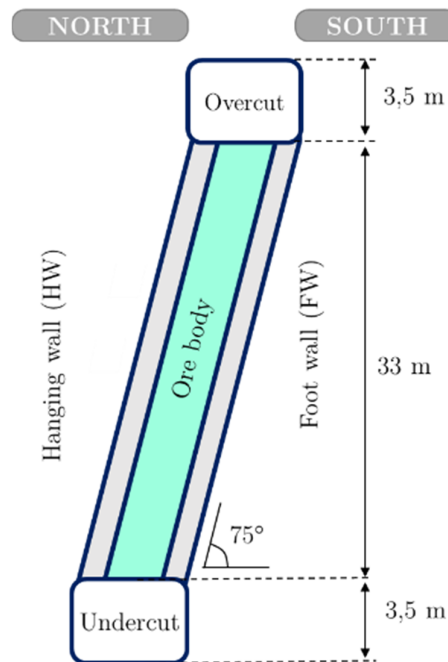

Figure 1. Sublevel cross section

2.2. Finite Element Numerical Approach

A numerical approach using the finite element method was adopted in this study to simulate the development of the relaxation zone around sublevel stope. A representative two-dimensional geometric model was designed. The model

reproduces a typical cross-section of an underground mining operation exploited by the undercut sublevel method, with varying dimensions and geometry according to the configurations studied. The boundary conditions were applied in such a way as to represent the in-situ stresses as a function of depth and the k ratio (horizontal stresses over vertical stresses).

The two-dimensional numerical model encompasses dimensions of 300 meters in width and 150 meters in height, encompassing an area approximately three times larger than the excavated sublevel open stope under investigation. The model is subjected to fixed boundary conditions along its lateral (left and right) and basal extents, effectively replicating clamped states. However, the superior model surface is rendered free, enabling the application of a uniformly distributed vertical stress across this exposed facet. The magnitude of the applied vertical stress is calculated explicitly for each modeled scenario, contingent upon the depth at which the sublevel open stope is situated within the rock mass. This configuration aims to replicate the in-situ stress conditions and associated deformation response within the vicinity of the underground excavation.

The behavior of the rock mass was modeled using an elastoplastic constitutive law, with the generalized Hoek-Brown failure criterion [18].

2.3. Hoek-Brown Failure Criterion

The empirical Hoek-Brown failure criterion, widely used in mining geotechnics, was employed to delineate potential relaxation zones around the excavations. This criterion, initially developed for intact rock, was extended to fractured rock masses by introducing the Geological Strength Index (GSI) to account for the influence of discontinuities. The rock mass constants *mb*, *s*, and *a* are determined from the GSI or RMR, the uniaxial compressive strength of the intact rock σc, and a disturbance factor *D* related to the excavation conditions [19].

The influence of blast damage on the near surface rock mass properties has been taken into account in the 2002 version of the Hoek-Brown criterion (Hoek, Carranza-Torres and Corkum, 2002) as follows:

$$m_b = m_i . e^{\frac{GSI-100}{24-14D}}$$

S and a are constants for the rock mass given by the following relationships:

$$s = e^{\frac{GSI-100}{9-3D}}$$

$$a = \frac{1}{2} + \frac{1}{6}\left(e^{-\frac{GSI}{15}} - e^{-\frac{20}{3}}\right)$$

$$GSI = RMR_{76}$$

The safety factor is given by the following equation:

$$SF = \frac{\sigma'_3 + (m\sigma_{UCS}\sigma'_3 + s\sigma_{UCS})^a}{\sigma'_1}$$

Where:

m_b: The reduced value of the material

m_i: Intact rock constant

GSI: Geological Strength Index

σ_{UCS}: uniaxial compressive strength of the intact rock

D: Disturbance Factor

In the finite element models, elements whose principal stress ratio exceeds the Hoek-Brown (2002) criterion are considered plastified, thus delineating the potential relaxation zone.

2.4. Variable Input Parameters

To evaluate the influence of the different key parameters on the extent of the relaxation zone, a series of numerical simulations was carried out by varying the following parameters:

- Excavation depth: from 100 to 900 m
- k ratio of horizontal to vertical stresses: from 1 to 2.5
- Rock mass quality (GSI/RMR): from 35 to 75%
- Foliation orientation: from 0° to 90° relative to the horizontal
- Foliation spacing: from 0.2 to 2 m
- Height of sublevels: from 10 to 40 m
- Width (span) of sublevels: from 3.5 to 9.5 m
- Inclination of sublevels: from 45° to 90° relative to the horizontal

A total of 425 distinct simulations were performed by combining different values of these input parameters. For each simulation, the extent of the relaxation zone was measured at the level of the hanging walls of the sublevel stope.

The rock mass encompassing the El Hammam mine is traversed by a pervasive schistosity that remains parallel to the mineralized vein, and consequently, parallel to the void created by the sublevel open stope excavation. The distinction between foliation and schistosity resides primarily

in the potential variability of mineralogical compositions across the discrete laminations. However, from the perspective of wallrock stability, these planar anisotropic fabrics exhibit analogous mechanical behavior and structural competency characteristics within the excavation boundaries.

Notwithstanding the potential mineralogical disparities between foliation and schistosity, their parallel orientations relative to the excavated stope suggest a uniform anisotropic response to the induced stress redistribution within the rock mass. Consequently, the stability assessments and reinforcement strategies employed for the excavation boundaries should consider the inherent structural weaknesses associated with these planar discontinuities, irrespective of their specific mineralogical compositions.

2.5. Development of Predictive Models

The results of the numerical simulations were then exploited to develop predictive models to estimate the extent of the relaxation zone as a function of the different input parameters. Two complementary approaches were implemented:

- **Multiple Regression Analysis:** This statistical technique aims to establish a linear or non-linear relationship between a dependent variable (here, the extent of the relaxation zone) and several independent variables (the input parameters) [20]. An iterative least-squares optimization procedure was used to determine the regression equation coefficients offering the best correlation with the simulated data. Distinct regression models were developed for each influential parameter or combination of parameters.

- **Artificial Neural Networks (ANNs):** This artificial intelligence approach is based on the training of an interconnected network of neurons to model complex relationships between input and output parameters. A multilayer perceptron (MLP) network with two hidden layers and an output layer was designed. The backpropagation algorithm was used to iteratively adjust the connection weights between neurons to minimize the error between predicted and simulated data values. In total, 72.2% of the data were used for network training, while 27.8% served for validation.

The accuracy and performance of the predictive models were evaluated by comparing predicted values to simulated data, using statistical metrics such as the Pearson correlation coefficient (R2) and graphical analysis of scatter plots. A comparative approach between multiple regression models and artificial neural networks allowed identifying the most robust method for predicting the extent of the relaxation zone as a function of the different input parameters.

The developed models were then analyzed to highlight the relative influence of the different key parameters on the extent of the relaxation zone. This analysis helped to identify general trends and the predominant parameters to be considered in the design of underground mining operations exploited by the undercut sublevel method.

3. Results and discussion
3.1. Effect of Depth and K Ratio on the Relaxation Zone

To assess the impact of depth on the shape and extent of the relaxation zone around sublevel stope [21], a series of eight finite element simulations was performed. These simulations considered an undercut sublevel with a width of 3.5 m and a height of 40 m, located at depths ranging from 200 to 900 m. Figure 2 shows the superposition of the relaxation zones obtained for the different simulated depths. The results reveal a progressive increase in the extent of the relaxation zone at the level of both hanging walls as depth increases. This trend is mainly attributable to the increase in vertical stress with depth.
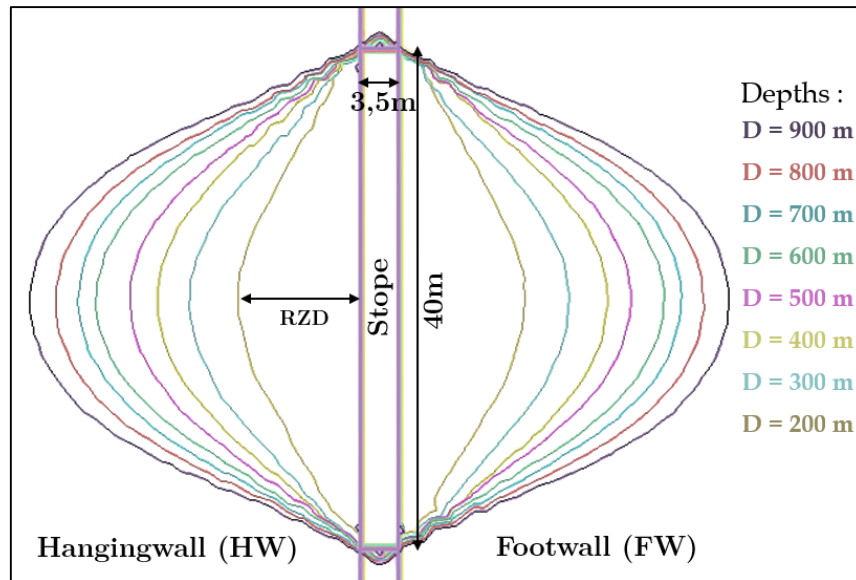
Figure .2: Superposition of relaxation zones at different depths.

During the excavation of an underground opening, the in-situ stresses undergo a disturbance and redistribution in the vicinity of the excavation. These stresses can be categorized as natural stresses (pre-existing) and stresses induced by the excavation. Natural stresses result mainly from the weight of the overburden (gravitational stress) and regional tectonic processes (crustal tectonic stress) [22]. These natural stresses tend to be isotropic. They are generally expressed in terms of principal stresses, with the maximum ($\sigma 1/\sigma 3$) and minimum ($\sigma 2/\sigma 3$) ratios of horizontal to vertical stresses denoted as k. In the studied region, the k ratio typically varies between 1 and 2.5 [22]. In-situ measurements have shown that this ratio tends to decrease with depth, as illustrated in Figure 3.

To evaluate the combined effect of depth and the k ratio on the extent of the relaxation zone at the level of the hanging walls, simulations were carried out on an identical geometric model at different depths and for different values of k. Table 1 presents the resulting relaxation distance values in each simulated scenario.
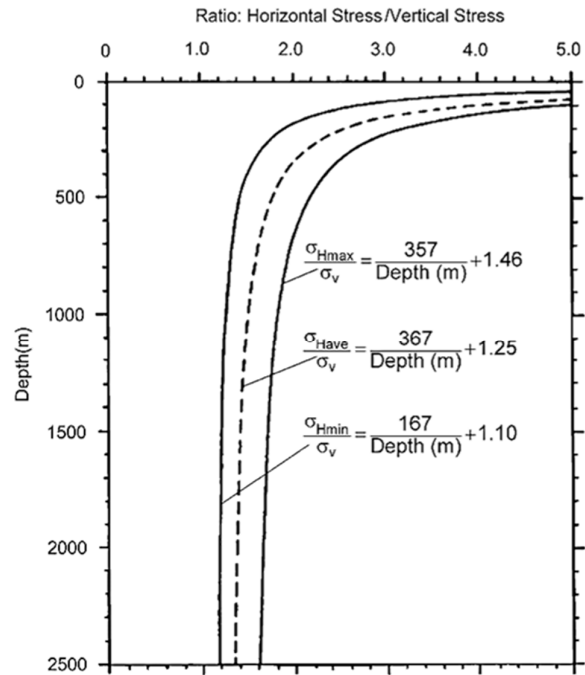

Figure 3. Variations of the in-situ stress ratio k as a function of depth [23].

$$\frac{\sigma_{Hmax}}{\sigma_v} = \frac{357}{Depth\ (m)} + 1.46$$

$$\frac{\sigma_{Have}}{\sigma_v} = \frac{367}{Depth\ (m)} + 1.25$$

$$\frac{\sigma_{Hmin}}{\sigma_v} = \frac{167}{Depth\ (m)} + 1.10$$

Table 1. Relaxation zone extent as a function of depth and k ratio.

K \ Depth (m)	200	300	400	500	600	700	800	900
1	11,5	15,9	19,2	21,8	24,24	26,6	28,68	30,9
1,5	11,6	16,13	19,2	21,9	24,31	26,7	28,75	30,92
2	11,6	16,23	19,24	21,97	24,33	26,71	28,77	30,98
2,5	11,61	16,24	19,32	21,98	24,5	26,72	28,86	31,06

The analysis of the results reveals that, for a given depth, the variation of the k ratio does not have a significant impact on the extent of the relaxation zone, with a maximum influence of 2%.

Figure 4 presents the simulated relaxation distances as well as the 3D surface fitted to the measured points using an analytical expression. This expression, proposed to determine the relaxation

zone as a function of depth and k ratio, is given by the following equation:

$R^2=0,98$

Where:

$$RZD = 8,83 + 47,88. e^{-0,5(G-H)}$$

$$G = \left[\frac{k, \cos(0\ 004) + Depth, \sin(0\ 004) - 25\ 25, \cos(0\ 004) - 1017\ 46, \sin(0\ 004)}{19\ 34}\right]^2$$

$$H = \left[\frac{-k, \sin(0\ 004) + Depth, \cos(0\ 004) + 25\ 25, \sin(0\ 004) - 1017\ 46, \cos(0\ 004)}{459\ 86}\right]^2$$
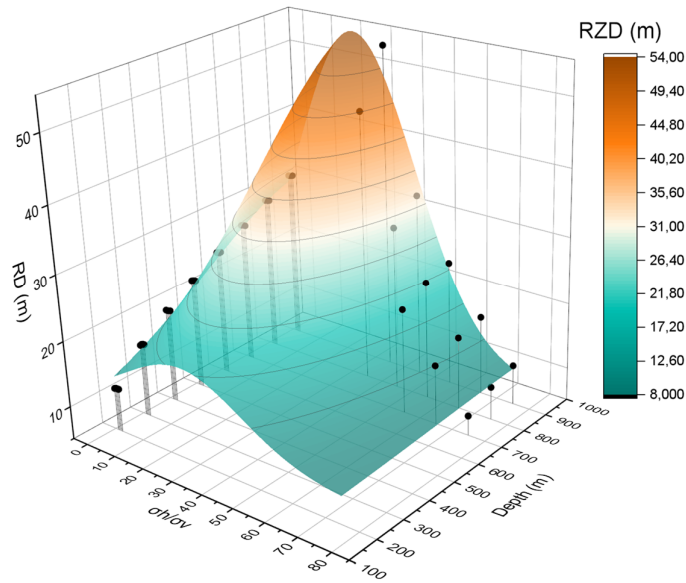

Figure 4. Simulated relaxation distances and 3D surface fitted to the measured points

The numerical simulations have thus highlighted the predominant role of depth on the extent of the relaxation zone around sublevel stope, while the influence of the in-situ stress ratio k proved relatively low under the studied conditions.

3.2. Effect of Rock Mass Quality

The quality of the rock mass plays a crucial role in the hanging wall stability of sublevel stope [24]. In the context of this study, the sublevels are excavated in a rock mass with highly variable quality. To assess the influence of this parameter on stability conditions, surveys were carried out in the upper and lower levels using the Rock Mass Rating (RMR) classification. On this basis, 45 finite element simulations were performed considering scenarios with RMR values ranging from 35% to 75%, for depths ranging from 100 to 900 m.
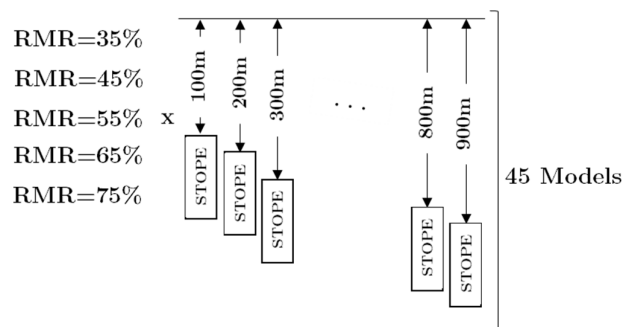

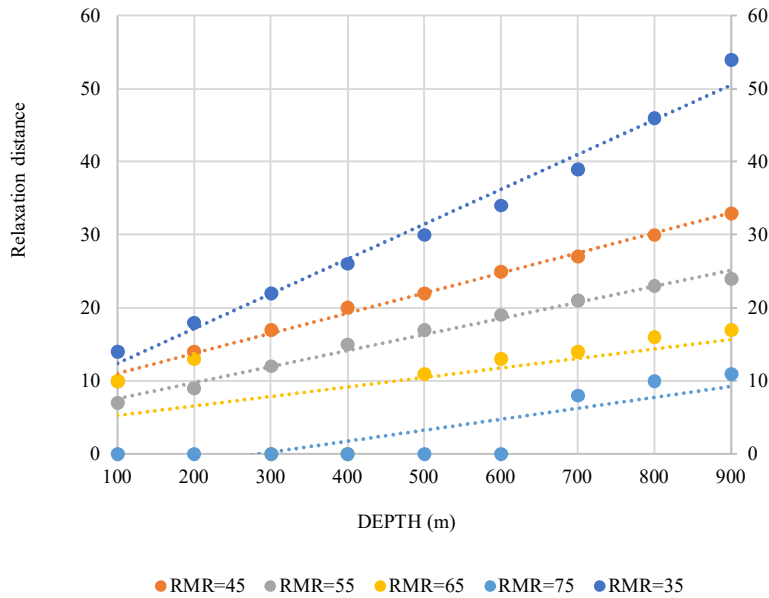**Figure 5. Stopes depth and RMR used in this analysis**

Figure 6. Relaxation distance as a function of rock mass quality (RMR) and sublevel depth.

To determine the combined effect of rock mass quality (RMR) and depth on the relaxation distance, an analytical expression was proposed, given by the following equation:

$$RZD = -8,62 + 8423,2.\,e^{-A} - 115,2.\,e^{-B} - 242752\,.\,e^{-C}$$

$R^2 = 0,94$

Where:

$$A = e^{\frac{-363\,59 - RMR}{-363\,59}}$$

$$B = e^{\frac{1699\,7 - Depth}{1398\,39}}$$

$$C = \left[e^{\frac{363\,59 + RMR}{363\,59}} + e^{\frac{1699\,7 - Depth}{1398\,39}} \right]$$

This expression, taking into account both RMR and depth, exhibits a high correlation with the simulated measurement points, with a coefficient of determination R² of 0.94, as shown in figure 7.

The results of the numerical simulations have thus highlighted the predominant role of rock mass quality, characterized by the RMR, on the extent of the relaxation zone around sublevel stope. A decrease in rock mass quality leads to a substantial increase in this zone, underscoring the importance of this parameter in ensuring hanging wall stability during the design of underground mining operations.

3.3. Impact of Geometric Parameters on Sublevel Stability

In the context of deep underground mining operations using the undercut sublevel method, the geometric design of the excavations is crucial to ensure the structural integrity of the hanging walls and guarantee safe and productive operating conditions [25]. The main morphological descriptors to consider are the vertical and horizontal dimensions of the excavation, as well as the inclination of the stope faces. The present study aims to conduct a rigorous parametric analysis to quantify the effects induced by these dimensional attributes on the extent of the relaxation zone at the level of the hanging walls.
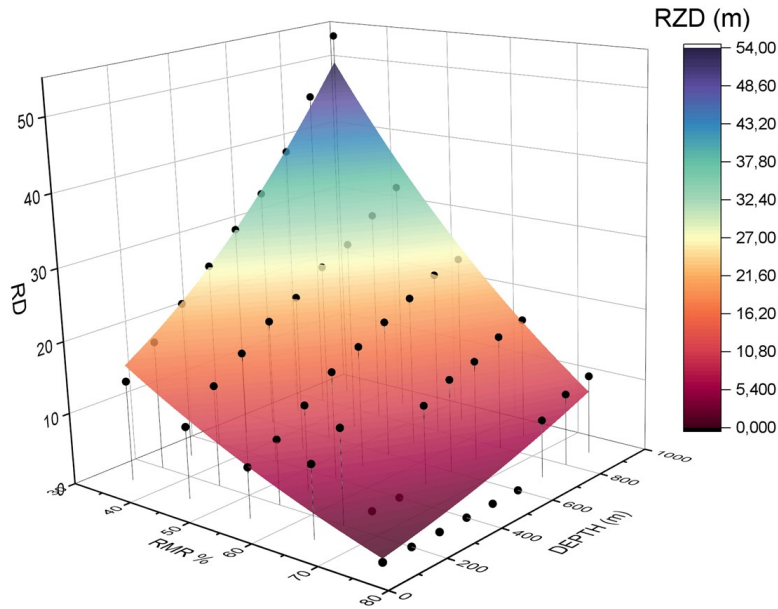
Figure 7. Simulated relaxation distances and 3D surface fitted as a function of RMR and depth.
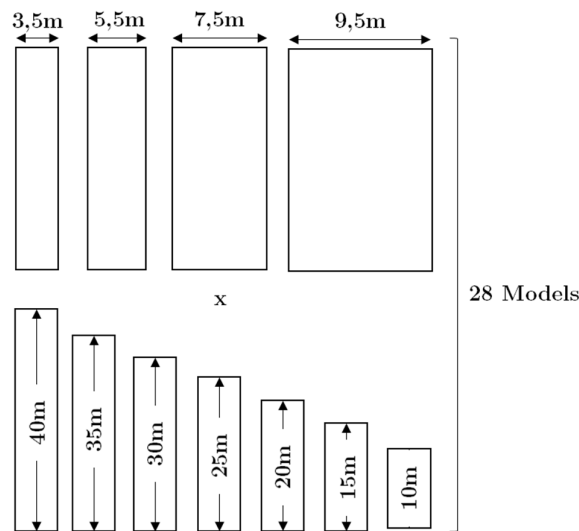

Figure 8. Stopes geometry used in this analysis

A complete numerical experiment plan was developed, covering 28 distinct configurations by varying the height of the sublevels from 10 to 40 m, the span from 3.5 to 9.5 m, and the inclination of the stopes faces from 45° to 90° relative to the horizontal. To isolate the influence of the geometric parameters, the depth was kept constant at 300 m, and the geomechanical properties of the rock mass were set to an RMR index of 60%. The values of the resulting relaxation distance in each scenario are presented in Table 2.

Table 2. La portée de la zone de relaxation en fonction de la hauteur et la largeur de l'ouvrage

Width (m)	Height (m)						
	10	15	20	25	30	35	40
3,5	5,72	7,4	9,35	10,89	12,29	15,04	15,83
5,5	6,27	7,91	9,71	11,71	13,54	15,54	16,01
7,5	6,3	8,06	10,03	11,91	13,64	15,58	17,5
9,5	6,36	8,43	10,5	12	13,95	15,82	17,58

The results of the numerical simulations revealed a clear correlation between the dimensions of the excavations and the extent of the relaxation zone at the level of the hanging walls. An empirical relationship was formulated to quantify this dependence:

$$RZD = 2{,}19 + 0{,}33.\,width + 0{,}29.\,height$$

$R^2 = 0{,}98$

where RZD represents the relaxation distance (in meters) at the level of the unstable hanging wall.

The plot of the proposed model superimposed on the measured points is presented in the following figure 9:
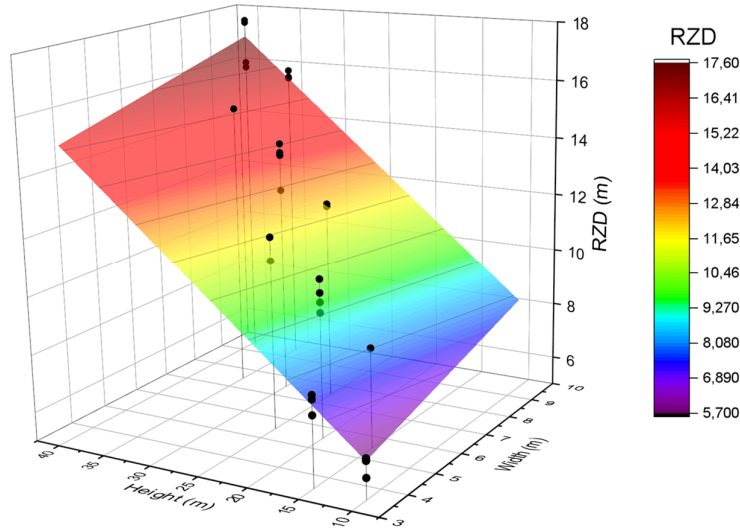

Figure 9. Distances de détente simulés et surface 3D ajustée aux points mesurés

This expression highlights the predominant impact of the vertical height and horizontal span of the sublevels on the extent of the relaxation zone. An increase in these parameters induces a more pronounced stress redistribution and amplification of the deconfinement phenomena within the surrounding rock mass. Excessive heights can lead to shear or toppling failures of the hanging walls, particularly in geological formations with low geomechanical competence.

Beyond the main geometric dimensions, other parameters also play a key role. Notably, the inclination of the stoping faces, i.e., the angle α of the stope face relative to the horizontal, also has a considerable impact [26, 27]. To quantify the impact of this slope on the relaxation distance at the level of the hanging walls of sublevel stope excavated in rock masses of different RMR qualities, we will consider the following cases:
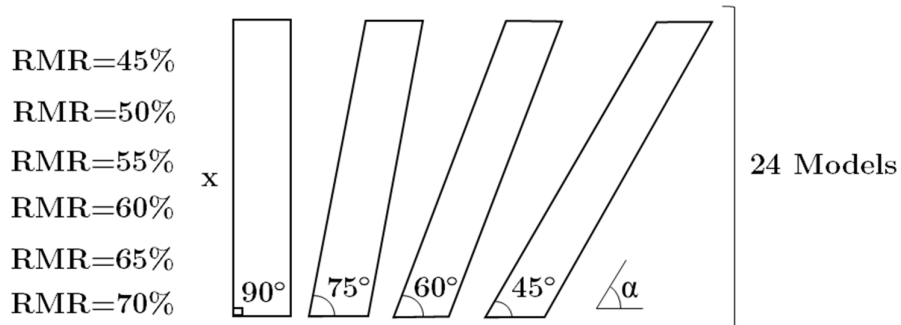

Figure 10. Stopes slope used in this analysis

a) α =90°   **b). α =75°**   **c) α =60°**   **d) α =45°**
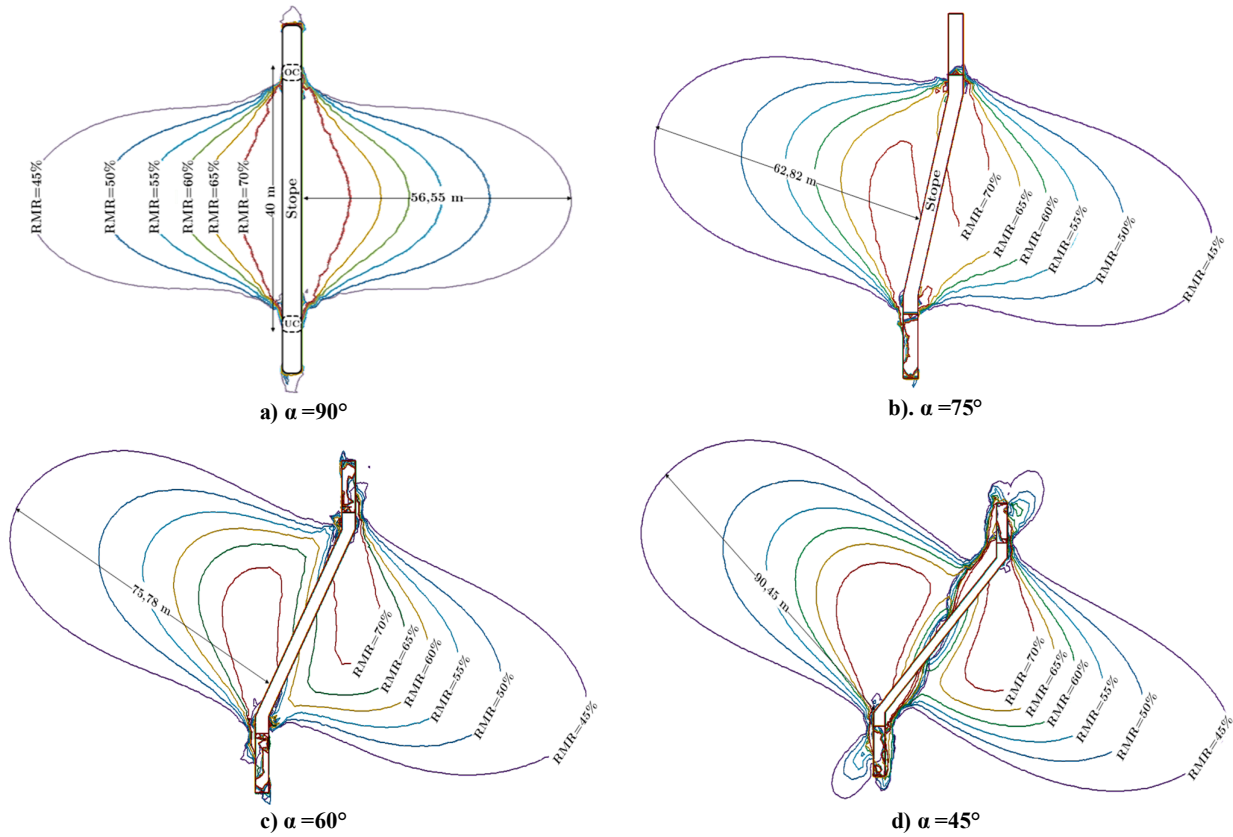
Figure 11. Superposition of relaxation zone limits as a function of the undercut sublevel slope.

The analysis of the superposition of the relaxation zone contours reveals that the instability arch increases with inclination. A sublevel inclined too far downwards favors planar failures along unfavorably oriented discontinuities. In contrast, an overly steep slope can lead to toppling or shear failures of the hanging walls.

For a given rock mass quality, the relaxation zone distance is very high in the most inclined sublevels. Furthermore, it is observed that this relaxation distance is greater at the level of the suspended or hanging wall, which is the focus of our study.
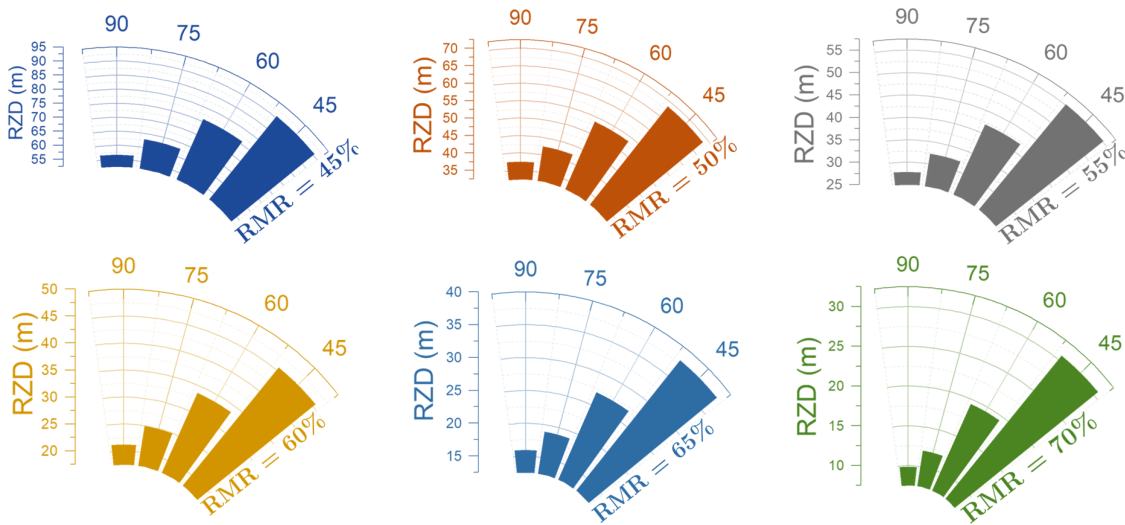

Figure 12. Polar diagram of relaxation distances according to RMR class

An expression was developed to estimate the relaxation distance as a function of the inclination α of the stoping faces and the geomechanical quality of the rock mass (RMR):

$$RZD = e^{-A}$$

$$R^2 = 0,98$$

Where:

$$A = 5,973 + 8,667 . \ln(RMR) - 1,837 . \ln(RMR)^2 + 0,151 . e^{-B}$$

$$B = e^{\left(-\frac{\sin(\alpha) - 20\,631}{-1\,636}\right)} - \left(\frac{\sin(\alpha) - 20\,631}{-1\,636}\right) + 1$$

3.4. Impact of schistosity on sublevel stope stability
3.4.1. Effect of the foliation orientation (β)

In geological formations exhibiting marked foliation, the relative orientation of structural discontinuities compared to the geometry of underground mine workings exerts a predominant influence on the stability regime of the rock walls [27]. The present study aims to characterize the effect of foliation orientation (β) on the extent of the detachment zone at the level of the hanging wall of excavations by undercut sublevel s, considering different dip angles (α) of the undercut faces.

A numerical simulation campaign using the finite element method was undertaken to reproduce the stress field induced in the foliated rock mass around the undercut sublevel s. In total, 45 distinct configurations were modeled by varying the foliation orientation β from 0° to 90° with respect to the horizontal, and the dip angle α of the undercut faces at 90°, 75° and 60°. In order to isolate the influence of structural parameters, the depth was kept constant at 300 m, and the geomechanical properties of the rock mass were set to an RMR index of 60%. The extent of the relaxation zone at the level of the unstable wall was delimited by applying the non-linear Hoek-Brown generalized failure criterion.

The superposition of the contours of the relaxation zones for the different simulated configurations has highlighted the evolution of the critical unconfined points as a function of the β orientation of the foliation. A lateral displacement and amplification of the extent of the relaxation

zone is observed when the orientation of the foliation approaches an unfavorable attitude with respect to the hanging wall.

The maximum relaxation distance occurs for an orientation β ≈ 75°, where the foliation planes can act as preferential sliding surfaces, thus promoting structural instabilities. Conversely, when the orientation of the foliation becomes quasi-perpendicular to the wall (β ≈ 15°), a configuration qualified as an "ideal massif", the relaxation distance is minimized. In this optimal structural configuration, the foliation discontinuities exert only a weak influence on the failure potential of the walls.

In order to quantify this dependence, an empirical relationship has been formulated to estimate the relaxation distance (RZD) as a function of the β orientation of the foliation and the α dip of the undercut faces:

$$RZD = -0,64 + 101 . e^E - 8,67 . e^F + 106,79 . e^H$$

$$R^2 = 0,98$$

Where:

$$E = \frac{\ln\left(\frac{\alpha}{16\,38}\right)^2}{-1\,64}$$

$$F = \frac{\ln\left(\frac{\beta}{75\,32}\right)^2}{-0\,051}$$

$$H = \frac{\ln\left(\frac{\alpha}{16\,38}\right)^2}{-1\,64} + \frac{\ln\left(\frac{\beta}{75\,32}\right)^2}{-0\,051}$$
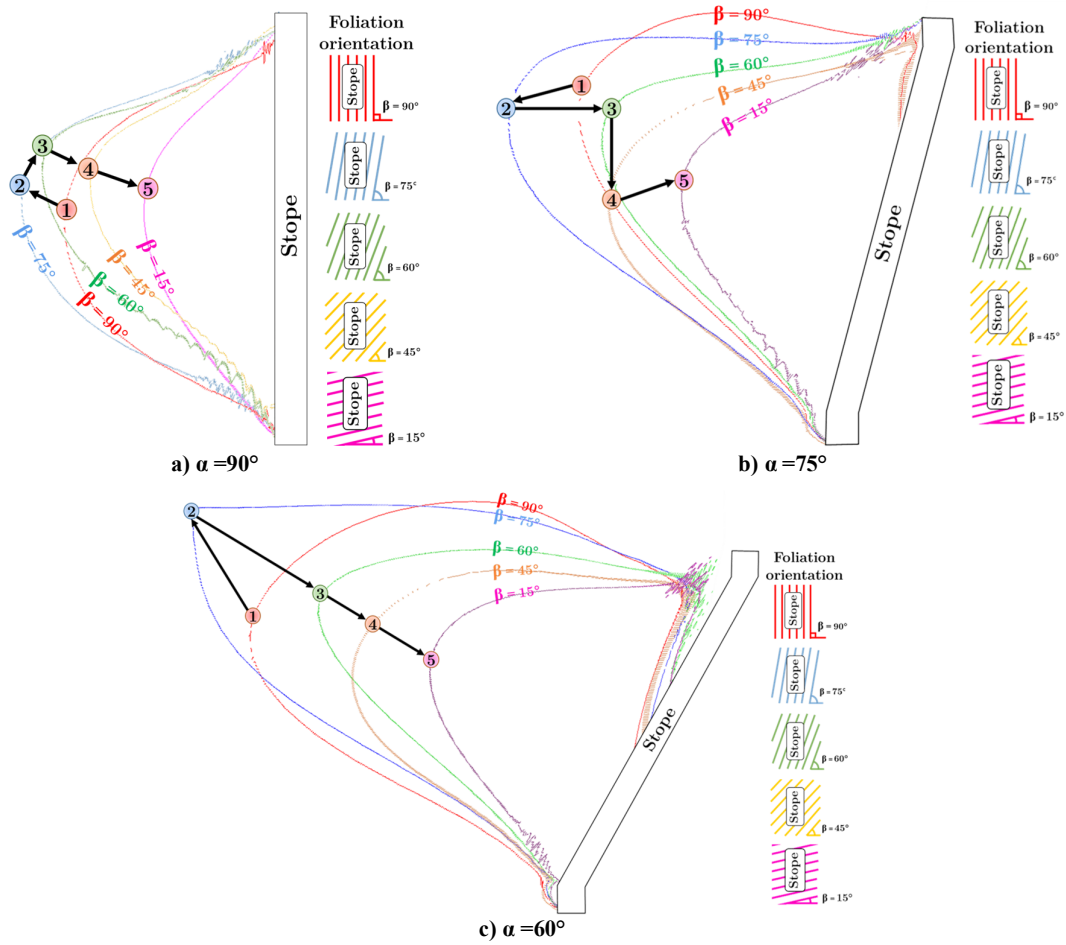
a) α =90°

b) α =75°

c) α =60°

Figure 13. Superposition of relaxation zones according to foliation orientation and dip of the stope

This proposed expression, adjusted with a determination coefficient R² of 0.98, allows predicting with good precision the impact of structural conditions on the geomechanical response at the level of the walls of undercut sublevel s. The plot of the proposed model superimposed on the measured points is presented in the figure 14:
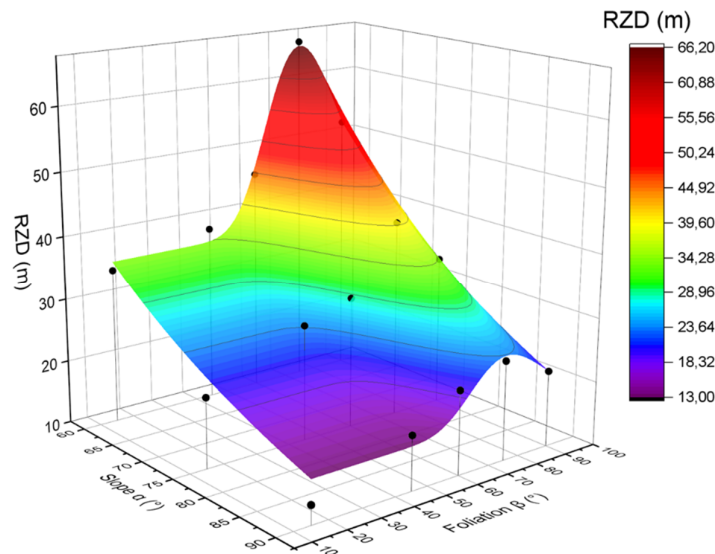

Figure 14. Simulated relaxation distances and 3D surface fitted to the measured points

3.4.2. Effect of the foliation spacing (Sp)

In rock masses exhibiting marked foliation, the spacing between the structural discontinuity planes represents a critical parameter for the stability of the walls of underground mining stopes. These spacing conditions the dimensions of the individual blocks constituting the rock mass, thus directly influencing its overall mechanical behavior [28].

In order to elucidate the impact of foliation spacing on the extent of the relaxation zone around the undercut sublevel s, a campaign of 12 numerical simulations was undertaken. Different configurations were evaluated considering spacings of 0.2 m, 0.6 m, 1 m and 2 m for structures with dip angles α of 90°, 60° and 45°.
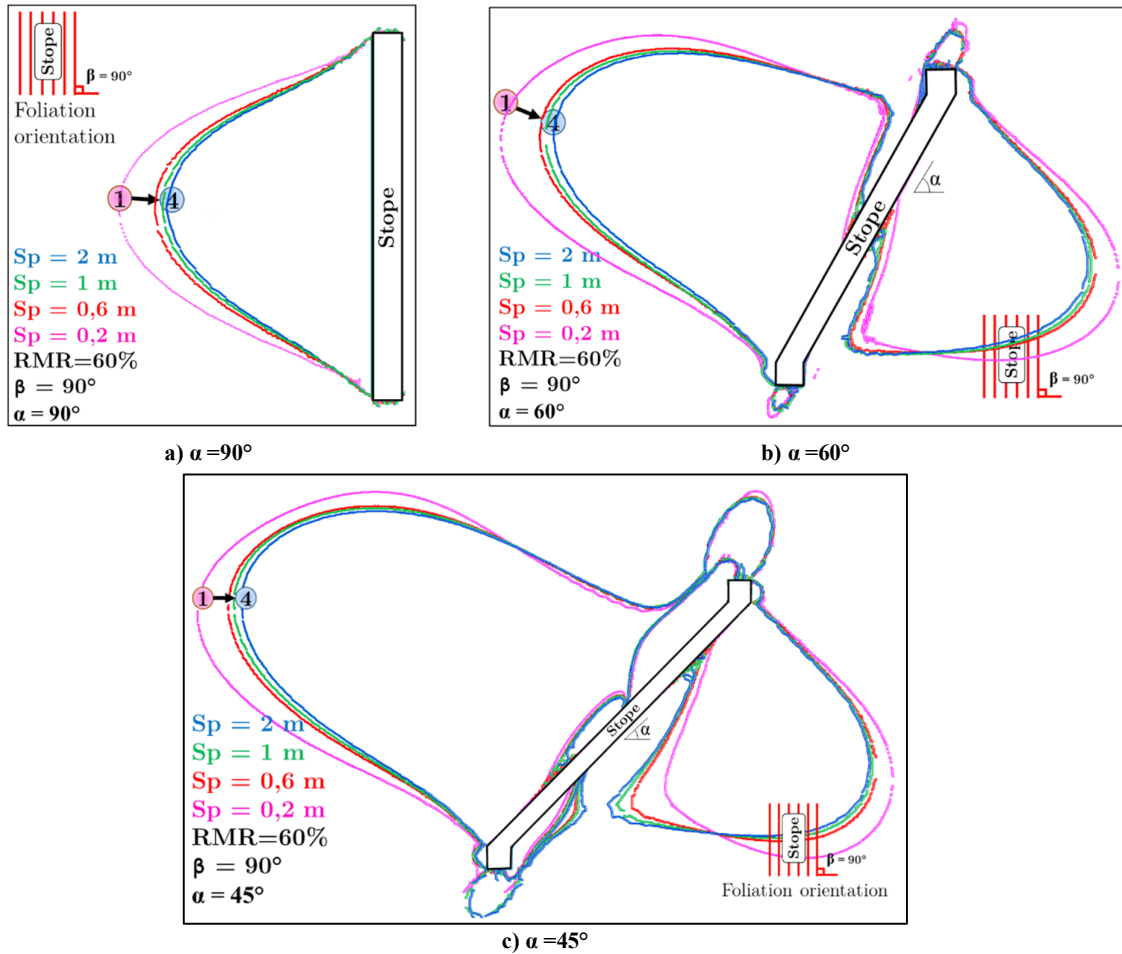

Figure 15. Superposition of relaxation zones according to foliation spacing and dip of the excavation

The analysis of the superposition of the relaxation zones associated with each schistosity spacing reveals a distinctive trend. As the joint spacing increases, the relaxation arc tightens more around the excavation. In other words, an increase in spacing improves the stability of the walls. This phenomenon can be explained by the fact that thicker strata behave like a more resistant rock slab. The increase in thickness of this slab results in a reinforcement of its structural resistance.

In order to quantify this relationship, a robust predictive model has been developed to estimate the relaxation distance as a function of the schistosity joint spacing (Sp) and the dip of the undercut sublevel (α):

$$RZD = 22,04 + 251 . e^{\frac{Sp}{2,08} - \frac{\alpha}{24,25}}$$

$R^2 = 0,98$

This empirical model, validated by a high correlation with the simulated data, allows accurately predicting the extent of the relaxation zone by taking into account these two determining structural parameters. The plot of the proposed model superimposed on the measured points is presented in figure 16.
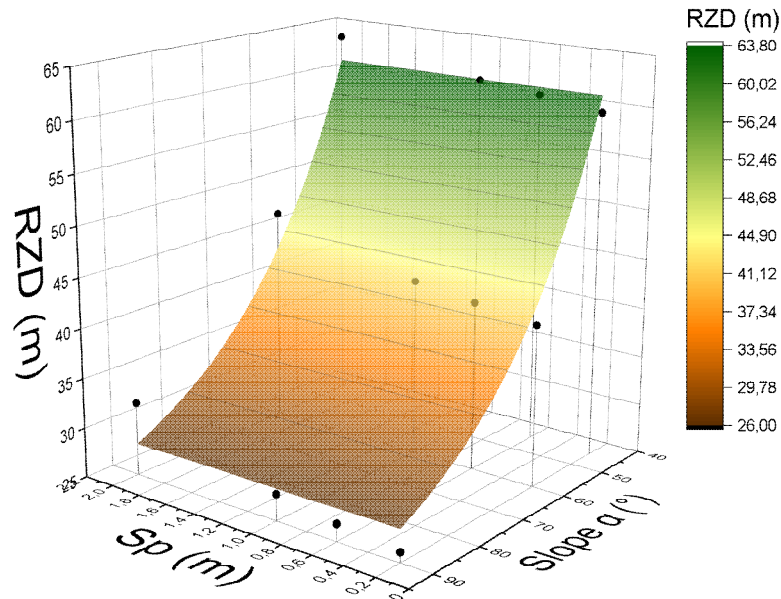
Figure 16. Simulated relaxation distances and 3D surface fitted to the measured points

The results obtained highlight the importance of considering the foliation spacing in the design of underground mine workings exploited by the undercut sublevel method. A larger joint spacing favor the stability of the walls by reducing the extent of the relaxation zone.

3.5. Artificial Neural Network (ANN)

Artificial neural networks (ANNs) are components of artificial intelligence techniques designed to simulate the human brain while analyzing and processing information through many interconnected neurons. Based on this knowledge, ANNs have recently been introduced and extended to achieve numerous successes in various engineering fields. The automatic learning capabilities of ANNs improve their performance in solving difficult and complex problems regardless of the amount of data. An artificial neural network consists of hundreds of thousands of artificial neurons interconnected by nodes used as processing units. The processing units are divided into input and output units. Based on the internal weight system, the input units receive the information. Consequently, the neural network in the hidden layer attempts to learn about the information presented to produce an output report. Error backpropagation, abbreviated as backpropagation, is used in the artificial neural network as a learning rule to minimize error values. Then, they produce accurate results for the output reports. Artificial neural networks are primarily

categorized into feedforward neural networks and feedback (recurrent) neural networks. In the feedforward neural network, signals move directly from input to output in a single direction. Whereas in feedback neural networks, signals can move in both directions while network connections can form one or more loops. A feedforward neural network (FFNN) is the first and most common type of artificial neural network. An FFNN can develop through a single layer, a multilayer perceptron (MLP), and a radial basis function (RBF) [29, 30].

3.5.1. The Multilayer Perceptron (MLP)

The Multilayer Perceptron (MLP) is the most popular and widely used type of feedforward neural network (FFNN). Typically, the MLP consists of three layers: an input layer, a hidden layer, and an output layer. The input signals xi (i = 1,2 … n) are distributed to the neurons of a hidden layer by the neurons of the input layer. Each neuron in the hidden layer (j) weights its signals with the respective connection strengths (wji) and then sums the received signal (xi). Finally, the outputs yj will be calculated in the hidden layer by the neurons as a summation function (f) [31]:

$$y_i = f(\sum_{i=1}^{n} w_{ji} x_i)$$

Similarly, the output of the neurons is calculated in the output layer. The multilayer perceptron (MLP) training algorithm is adopted by the

backpropagation algorithm as a supervised learning method. The training is applied based on the connection weight between the neurons [32].
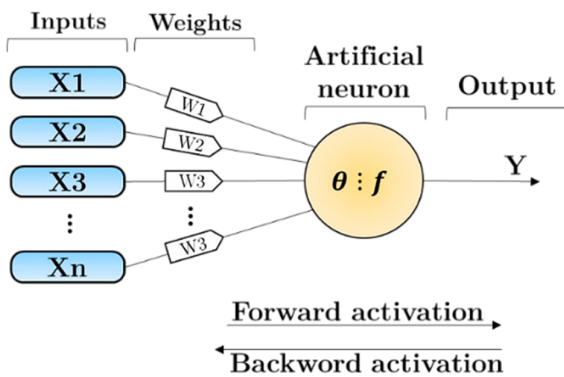

Figure 17. Process in multilayer perceptron

3.5.2. Applications of ANN

In recent years, the artificial neural network (ANN) technique has generated a real technological revolution in the mining field and related branches of engineering. In addition to their remarkable ability to solve complex engineering problems, ANNs offer a predictive potential applicable to a wide range of applications in the mining sector [33].

Neural networks are now essential digital tools for various mining operations, such as geophysical data interpretation, ore processing, equipment selection, underground mining method selection, blasting operation optimization, environmental impact assessment of mine blasts, or even calculating the net present value of projects [34].

Thanks to their automatic learning capability, ANNs can efficiently process and analyze massive and complex data sets, thus overcoming the limitations of conventional methods. Their interconnected network architecture allows them to detect and model nonlinear relationships and subtle trends, often difficult to discern through traditional analytical approaches.

In the context of this research, a robust predictive model of the relaxation zone distance around undercut sublevel s has been developed using an artificial neural network. This model was trained based on 425 finite element simulations carried out, taking into account six key input parameters: RMR, height, dip, width, depth, and the ratio of horizontal to vertical stresses (k).
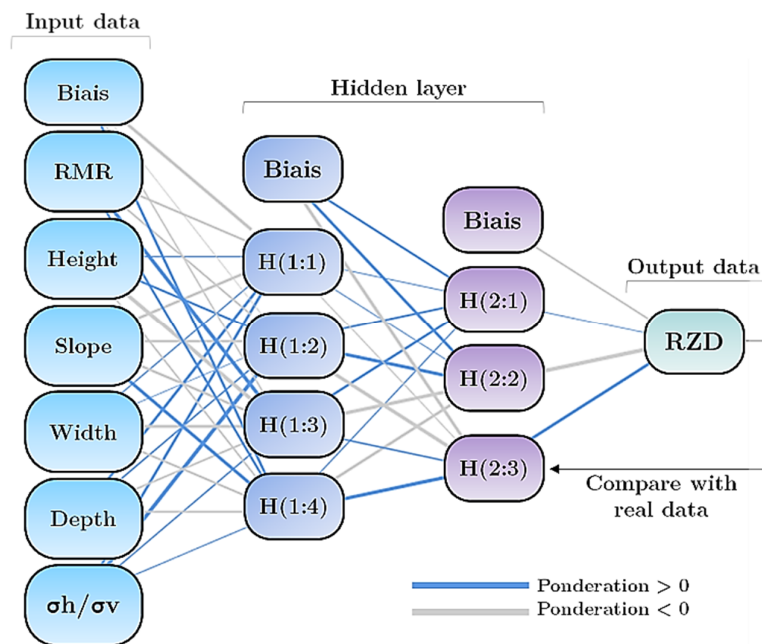

Figure 18. Artificial neural network architecture used in this study

The proposed network architecture includes two hidden layers activated by a hyperbolic tangent function, comprising four and three neurons, respectively. The learning process was performed by feedforward backpropagation, allowing the network to iteratively adjust its connection weights to minimize the error between predictions and observations.

Table 3. The input and output parameters used in ANN

	Parameter	Mean	Minimum	Maximum	Median
Inputs	RMR (%)	55	35	75	55
	Height (m)	29,3	10	40	30
	Slope α (°)	74,22	45	90	75
	Width (m)	5,26	3,5	9,5	5,5
	Depth (m)	339	100	900	300
	k	1,05	1	2,5	1
Output	RZD (m)	18,12	4,55	54	16,27

In the development of the predictive model for the relaxation zone distance, a rigorous set of techniques was implemented for the processing and analysis of the collected observations. Out of the 425 numerical simulations performed, a representative sample of 307 cases (72.2%) was dedicated to training the artificial neural network. The remaining 118 cases (27.8%) were reserved for the model validation phase.
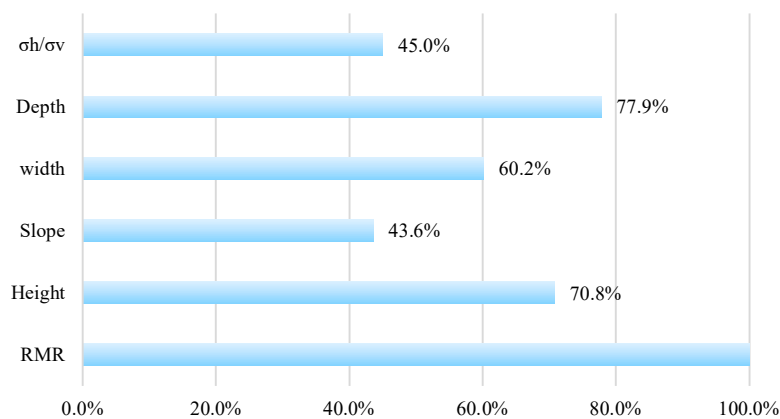
Figure 19. Normalized Importance of the ANN model

The normalized importance of the ANN model depicted in Figure 19 elucidates the preeminent role of the rock mass quality in governing the extent of the relaxation zone. The depth parameter emerges as the second most influential factor, exhibiting a normalized importance of approximately 78%. Geometric parameters such as the height, width, and inclination of the sublevels also exhibit notable, albeit relatively lesser, influence. Notably, the horizontal-to-vertical stress ratio (k) appears to have a relatively low impact.

The application of the artificial neural network methodology to predict relaxation distances revealed remarkable performance. A high Pearson correlation coefficient of $R^2 = 0.97$ was obtained between the values predicted by the model and the values actually measured during the simulations. This result attests to the network's ability to effectively capture the complex relationships between the different input parameters and the relaxation distance.

To visually assess the quality of the developed model, a graphical representation comparing the predicted values to the measured values was constructed. This in-depth graphical analysis allows for an intuitive appreciation of the model's performance.
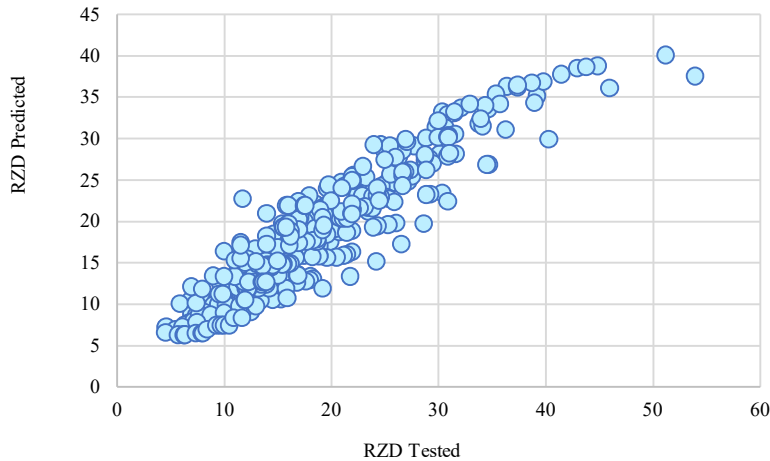
Figure 20. Comparison of predicted and measured values by the ANN method

Examination of the scatter plot presented in figure 20 reveals a marked tendency for the predicted values to align around the line y = x, representing perfect agreement between predictions and measurements. This arrangement suggests a close correspondence between the model's results and the actual observations, thus attesting to the very acceptable accuracy achieved by the artificial neural network approach. To evaluate the reliability and robustness of the predictive model based on neural networks, a comparative approach with the classical multiple regression method was adopted. The following regression model was proposed to estimate the relaxation zone distance:

$$RZD = 23 - 0{,}53.RMR + 0{,}47.H - 0{,}18.\alpha + 2.W + 0{,}023.D + 5{,}6.k$$

Wh re :

- H: heigh
- α : Stope slope

- W: width
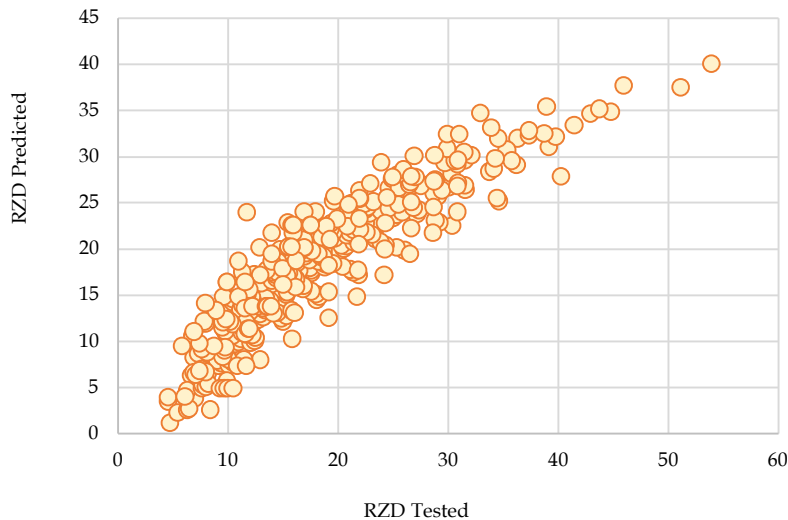- D: dept
- K : stress ratio

Figure 21. Comparison of predicted and measured values by the multiple regression method

The graphical analysis of the values predicted by the multiple regression model reveals a satisfactory accuracy, with a correlation coefficient $R^2 = 0.89$. However, the scatter plot presented in figure 20 shows a more significant dispersion around the line $y = x$, compared to the neural network model. The direct comparison of the performances of the two models presented in figure 22 highlights the superiority of the artificial neural network approach, with a higher correlation coefficient ($R^2 = 0.97$) than that of the multiple regression model ($R^2 = 0.89$). Furthermore, the visual analysis confirms that the ANN model fits more closely to the measured data, thus reinforcing its relevance and reliability compared to the regression method.
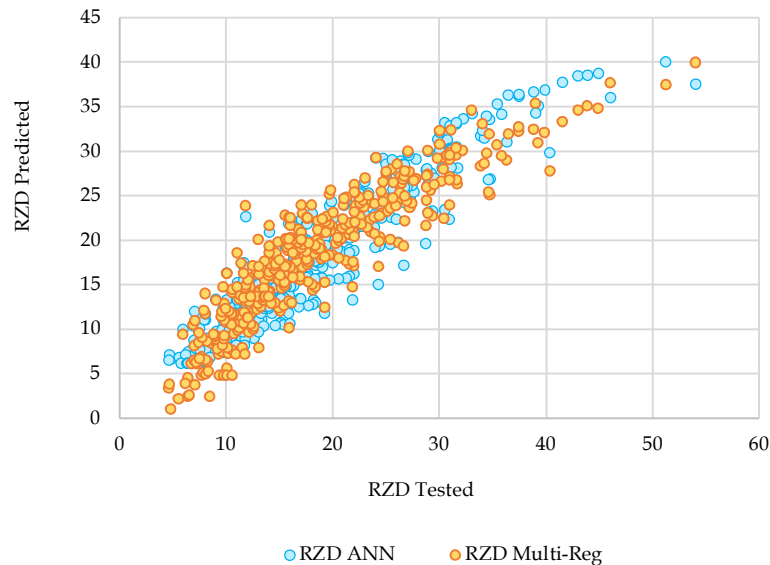

Figure 22. Comparison of predicted and measured values by the ANN and multiple regression models

These results demonstrate the potential of artificial neural networks to accurately model complex phenomena in mining engineering. Their ability to capture nonlinear relationships and efficiently process massive data sets offers promising new perspectives for addressing the challenges of underground mining, including predicting excavation stability, optimizing blasting operations, and managing geotechnical risks. However, it is important to note that ANNs do not replace conventional approaches but complement them judiciously. Their use should be part of a rigorous approach, ensuring a thorough understanding of the underlying phenomena and ensuring a prudent interpretation of the results obtained.

4. Conclusions

This study has provided an in-depth analysis of the relaxation zone around undercut sublevel s in underground mines, focusing on the influence of various key parameters. A numerical approach using the finite element method, combined with the Hoek-Brown failure criterion, has made it possible to delimit the potential relaxation zones according to various geometric configurations, geological conditions, and in-situ stress states.

The results of the numerical simulations have demonstrated the significant impact of depth on the extent of the relaxation zone, with a progressive increase in this zone as the depth increases. However, this effect is modulated by the ratio of horizontal to vertical stresses (k), which tends to decrease with depth under the studied conditions. The joint analysis of these two parameters has led to the development of a reliable predictive model to estimate the extent of the relaxation zone.

The quality of the rock mass, assessed by the Rock Mass Rating (RMR), has proven to be a determining factor. A decrease in RMR, reflecting a degradation in the quality of the rock mass, leads to a substantial increase in the relaxation zone around the undercut sublevel s. A predictive model combining depth and RMR has been proposed, offering high accuracy in estimating the extent of this zone.

The structural characteristics of the rock mass, such as the orientation and spacing of the foliation, have also been identified as influential parameters. Discontinuities unfavorably oriented with respect to the walls of the sublevel s can act as preferential

sliding surfaces, thus promoting instabilities. Conversely, a larger spacing between the foliation planes tends to improve wall stability.

Furthermore, the geometric parameters of the excavations, including the height, width (span), and dip of the undercut sublevel s, have a direct impact on the stress redistribution and, consequently, on the extent of the relaxation zone. Specific predictive models have been developed to quantify the influence of these geometric parameters.

Finally, an artificial intelligence approach based on artificial neural networks (ANNs) has been implemented to develop a global predictive model, taking into account all the key parameters studied. This ANN model has demonstrated high accuracy, with a correlation coefficient of 0.97 between the predicted and measured values. This superior performance compared to classical regression models underscores the potential of artificial intelligence techniques for addressing complex problems in mining engineering.

The predictive models developed in this study provide practical tools for optimizing the design of underground mine workings exploited by the sublevel stopping method. By considering the combined influence of various key parameters, these models will allow for improving the safety of mining operations and increasing the productivity of mining operations, while reducing the risks of instability and associated costs.

Further studies could be conducted to extend this analysis to other underground mining methods or to take into account additional factors, such as the mechanical properties of the rock mass or the dynamic effects related to mine blasts.

References

[1]. Hudson, J. A. (1993). Comprehensive rock engineering: principles, practice and projects. Volume 3. Rock testing and site characterization.

[2]. Soufi, A., Bahi, L., Ouadif, L., & Kissai, J. E. (2018). Correlation between rock mass rating, Q-system and rock mass index based on field data. In MATEC Web of Conferences (Vol. 149, p. 02030). EDP Sciences.

[3]. Soufi, A., Bahi, L., Ouadif, L., (2018). Adjusted anisotropic strength model for meta-siltstones and prediction of ucs from indirect tensile tests. *Int. J. Civ. Eng. Technol.*, *9*(7), 598-611.

[4]. Yaylacı, M., Abanoz, M., Yaylacı, E. U., Ölmez, H., Sekban, D. M., & Birinci, A. (2022). Evaluation of the contact problem of functionally graded layer resting on rigid foundation pressed via rigid punch by analytical and numerical (FEM and MLP) methods. *Archive of Applied Mechanics*, *92*(6), 1953-1971.

[5]. Yaylacı, M., Abanoz, M., Yaylacı, E. U., Ölmez, H., Sekban, D. M., & Birinci, A. (2022). The contact problem of the functionally graded layer resting on rigid foundation pressed via rigid punch.

[6]. Yaylacı, M., Şabano, B. Ş., Özdemir, M. E., & Birinci, A. (2022). Solving the contact problem of functionally graded layers resting on a HP and pressed with a uniformly distributed load by analytical and numerical methods. *Structural Engineering and Mechanics, An Int'l Journal*, *82*(3), 401-416.

[7]. Turan, M., Uzun Yaylacı, E., & Yaylacı, M. (2023). Free vibration and buckling of functionally graded porous beams using analytical, finite element, and artificial neural network methods. *Archive of Applied Mechanics*, *93*(4), 1351-1372.

[8]. Yaylacı, E. U., Öner, E., Yaylacı, M., Özdemir, M. E., Abushattal, A., & Birinci, A. (2022). Application of artificial neural networks in the analysis of the continuous contact problem. *Structural Engineering and Mechanics, An Int'l Journal*, *84*(1), 35-48.

[9]. Yaylacı, M., Yaylacı, E. U., Özdemir, M. E., Öztürk, Ş., & Sesli, H. (2023). Vibration and buckling analyses of FGM beam with edge crack: Finite element and multilayer perceptron methods.

[10]. Özdemir, M. E., & Yaylac, M. (2023). Research of the impact of material and flow properties on fluid-structure interaction in cage systems. *Wind and structures*, *36*(1), 31.

[11]. Yaylaci, E. U., Yaylaci, M., Ozdemir, M. E., Terzi, M., & Ozturk, S. (2023). Analyzing the mechano-bactericidal effect of nano-patterned surfaces by finite element method and verification with artificial neural networks. *Advances in nano research*, *15*(2), 165-174.

[12]. Yaylacı, M., Şabano, B. Ş., Özdemir, M. E., & Birinci, A. (2022). Solving the contact problem of functionally graded layers resting on a HP and pressed with a uniformly distributed load by analytical and numerical methods. *Structural Engineering and Mechanics, An 'nt'l Journal*, *82*(3), 401-416.

[13]. Sarfarazi, V., Haeri, H., Fatehi Marji, M., Saeedi, G., & Namdarmanesh, A. (2023). Investigation of Shear Properties of Open Non-persistent Latitudinal Discontinuities of Same Level. *Journal of Mining and Environment*, *14*(4), 1361-1371.

[14]. Rezaei, A., Sarfarazi, V., Babanouri, N., Omidi Manesh, M., & Jahanmiri, S. (2023). Failure Mechanism of Rock Pillar Containing Two Edge Notches: Experimental Test and Numerical Simulation. *Journal of Mining and Environment*, *14*(3), 961-971.

[15]. Omidi Manesh, M., Sarfarazi, V., Babanouri, N., & Rezaei, A. (2023). Investigation of External Work, Fracture Energy, and Fracture Toughness of Oil Well

Cement Sheath using HCCD Test and CSTBD Test. *Journal of Mining and Environment*, 14(2), 619-634.

[16]. Mortezaie, R., Mohammadi, S. D., & Sarfarazi, V. (2022). Preparation of Heterogeneous Rock-Like Samples Containing Non-Persistent Notch; Different Layout. *Journal of Mining and Environment*, 13(4), 1139-1157.

[17]. Fu, J., Safaei, M. R., Haeri, H., Sarfarazi, V., Fatehi Marji, M., Xu, L., & Arefnia, A. (2022). Experimental investigation on deformation behavior of circular underground opening in hard soil using a 3D physical model. *Journal of Mining and Environment*, 13(3), 727-749.

[18]. Kumar, H., Deb, D., & Chakravarty, D. (2017). Design of crown pillar thickness using finite element method and multivariate regression analysis. *International Journal of Mining Science and Technology*, 27(6), 955-964.

[19]. Liu, J., Lu, P., & Zhang, L. (2022). Influence of section shape and buried depth on rock loosening zone around underground roadway in coal mine. *ACS omega*, 7(38), 34296-34308.

[20]. Fávero, L. P., Belfiore, P., & de Freitas Souza, R. (2023). Data science, analytics and machine learning with R. Academic Press.

[21]. Xiang-Hui, Q. I. N., Peng, Z., Cheng-Jun, F. E. N. G., Wei-Feng, S. U. N., Cheng-Xuan, T. A. N., Qun-Ce, C. H. E. N., & You-Ru, P. E. N. G. (2014). In-situ stress measurements and slip stability of major faults in Beijing region, China. *Chinese Journal of Geophysics*, 57(4), 415-430.

[22]. Herget, G. (1987, February). Stress assumptions for underground excavations in the Canadian Shield. In *International Journal of Rock Mechanics and Mining Sciences & Geomechanics Abstracts* (Vol. 24, No. 1, pp. 95-97). Pergamon.

[23]. Zhao, X., & Zhou, X. (2022). Design method and application of stope structure parameters in deep metal mines based on an improved stability graph. *Minerals*, 13(1), 2.

[24]. Henning, J. G., & Mitri, H. S. (2007). Numerical modelling of ore dilution in blasthole stoping. *International Journal of Rock Mechanics and Mining Sciences*, 44(5), 692-703.

[25]. Yao, X., Allen, G., & Willett, M. (1999). Dilution evaluation using cavity monitoring system at HBMS—trout lake mine. In Proceeding of the 101st CIM annual general meeting, Calgary.

[26]. Diederichs, M. S. (2000). Instability of hard rockmasses, the role of tensile damage and relaxation.

[27]. Pérez-Rey, I., Moreno, J., & Muñiz-Menéndez, M. (2021, August). The role of joint spacing on the stability analysis of wedge failures. In *IOP Conference Series: Earth and Environmental Science* (Vol. 833, No. 1, p. 012095). IOP Publishing.

[28]. Moayedi, H., Mosallanezhad, M., Rashid, A. S. A., Jusoh, W. A. W., & Muazu, M. A. (2020). A systematic review and meta-analysis of artificial neural network application in geotechnical engineering: theory and applications. *Neural Computing and Applications*, 32, 495-518.

[29]. Koopialipoor, M., Fahimifar, A., Ghaleini, E. N., Momenzadeh, M., & Armaghani, D. J. (2020). Development of a new hybrid ANN for solving a geotechnical problem related to tunnel boring machine performance. *Engineering with Computers*, 36, 345-357.

[30]. Al-Shamisi, M. H., Assi, A. H., & Hejase, H. A. (2013). Artificial neural networks for predicting global solar radiation in Al Ain city-UAE. *International journal of green energy*, 10(5), 443-456.

[31]. Riedmiller, M. (1994). Advanced supervised learning in multi-layer perceptrons—from backpropagation to adaptive learning algorithms. *Computer Standards & Interfaces*, 16(3), 265-278.

[32]. Trivedi, R., Singh, T. N., Mudgal, K., & Gupta, N. (2014). Application of artificial neural network for blast performance evaluation. *International Journal of Research in Engineering and Technology*, 3(5), 564-574.

[33]. Wang, X., Lu, H., Wei, X., Wei, G., Behbahani, S. S., & Iseley, T. (2020). Application of artificial neural network in tunnel engineering: A systematic review. *IEEE Access*, 8, 119527-119543.

[34]. Nikafshan Rad, H., Bakhshayeshi, I., Wan Jusoh, W. A., Tahir, M. M., & Foong, L. K. (2020). Prediction of flyrock in mine blasting: a new computational intelligence approach. *Natural Resources Research*, 29, 609-623.

تجزیه و تحلیل عددی و مدل‌سازی پیش‌بینی با استفاده از هوش مصنوعی منطقه آرامش در اطراف دیوار آویزان ایستگاه‌های باز زیرسطحی در معادن زیرزمینی

امین صوفی*، یوسف زرادی، محمد سوئیسی، لطیفه اوادیف و انس بهی

دانشگاه محمد پنجم در رباط، مراکش

* نویسنده مسئول مکاتبات: amine.soufi@outlook.com

چکیده:

هدف از این مطالعه تجزیه و تحلیل کامل منطقه آرامش در حال توسعه در اطراف توقفگاه‌های زیرسطحی در معادن زیرزمینی و شناسایی پارامترهای اصلی کنترل کننده وسعت آن است. یک رویکرد عددی مبتنی بر روش اجزای محدود، همراه با معیار شکست هوک-براون، برای شبیه‌سازی پیکربندی‌های هندسی مختلف، شرایط زمین‌شناسی و حالت‌های تنش درجا اجرا شد. در مجموع ۴۲۵ شبیه‌سازی با عمق متغیر، نسبت تنش افقی به عمودی (k)، کیفیت توده سنگ (RMR)، جهت‌گیری و فاصله‌گذاری برگ‌ها و همچنین ارتفاع، عرض و شیب سطوح فرعی انجام شد. نتایج توسعه مدل‌های پیش‌بینی قوی را با استفاده از تکنیک‌های تحلیل رگرسیون و شبکه‌های عصبی مصنوعی (ANN) برای تخمین وسعت منطقه آرامش به عنوان تابعی از پارامترهای ورودی مختلف، فعال کرد. نشان داده شد که عمق و نسبت k به طور قابل توجهی بر وسعت منطقه آرامش تأثیر می گذارد. علاوه بر این، کاهش کیفیت توده سنگ منجر به افزایش قابل توجهی در این ناحیه می شود. ویژگی‌های ساختاری مانند جهت‌گیری شاخ و برگ و فاصله نیز نقش تعیین‌کننده‌ای دارند. در نهایت، پارامترهای هندسی حفاری‌ها، به ویژه ارتفاع، عرض و شیب سطوح فرعی، مستقیماً بر توزیع مجدد تنش و وسعت منطقه آرامش تأثیر می‌گذارند. مدل کلی ANN، با در نظر گرفتن تمام این پارامترهای کلیدی، دقت بالایی با ضریب همبستگی ۰.۹۷ از خود نشان داد. این مدل‌های پیش‌بینی ابزارهای ارزشمندی برای بهینه‌سازی طراحی عملیات استخراج زیرزمینی، بهبود ایمنی عملیاتی و افزایش بهره‌وری ارائه می‌دهند.

کلمات کلیدی: ایستگاه فرعی، منطقه آرامش، پایداری دیوار معلق، مدل‌سازی عددی، تحلیل اجزای محدود.